

A Switch Architecture for Time-Triggered Transmission with Best-Effort Delivery

Zonghui Li, Wenlin Zhu, Kang G. Shin, *Life Fellow, IEEE*, Hai Wan, Xiaoyu Song, *Senior Member, IEEE*, Dong Yang, *Senior Member, IEEE*, and Bo Ai, *Fellow, IEEE*

Abstract—In Time-Triggered (TT) or time-sensitive networks, the transmission of a TT frame is required to be scheduled at a precise time instant for industrial distributed real-time control systems. Other (or best-effort (BE)) frames are forwarded in a BE manner. Under this scheduling strategy, the transmission of a TT frame must wait until its scheduled instant even if it could have been transmitted sooner. On the other hand, BE frames are transmitted whenever possible but may miss deadlines or may even be dropped due to congestion. As a result, TT transmission and BE delivery are incompatible with each other.

To remedy this incompatibility, we propose a synergistic switch architecture (SWA) for TT transmission with BE delivery to dynamically improve the end-to-end (e2e) latency of TT frames by opportunistically exploiting BE delivery. Given a TT frame, the SWA generates and transmits a cloned copy with BE delivery. The first frame arriving at the receiver device is delivered with a configured jitter and the other copy ignored. So, the SWA achieves shorter latency and controllable jitter, the best of both worlds. We have implemented SWA using FPGAs in an industry-strength TT switches and used four test scenarios to demonstrate SWA's improvements of e2e latency and controllable jitter over the state-of-the-art TT transmission scheme.

Index Terms—synergistic switch architecture (SWA), dynamic latency improvement, controllable jitter, time-sensitive networking, industrial real-time control, FPGAs

I. INTRODUCTION

IN the past decade, Ethernet has been increasingly used/deployed in industrial distributed real-time control systems [1], [2]. However, the conventional Ethernet delivers frames in a best-effort (BE) manner without accounting for time-critical properties for industrial control tasks. Industrial Ethernet [3] is a set of new solutions that integrate industrial control networks and standard Ethernet. The time-triggered (TT) communication paradigm [4] is a cost-efficient solution for Industrial Ethernet. Time-critical frames for industrial control functions, called *TT frames*, are statically scheduled for transmission at precise time instants [5]. Meanwhile, the

other (called *BE*) frames are forwarded with BE delivery of the standard Ethernet. We call such networks with a TT communication paradigm *TT networks* [6].

Two typical networks for Industrial Ethernet fall into the category of TT networks. One is *TTEthernet*, standardized as AS6802 [7] targeting the aerospace domain by the Society of Automotive Engineers (SAE) International Group. It defines a fault-tolerant synchronization strategy to build and maintain synchronized time in a distributed system including terminal systems and switches. TT schedulers [8]–[11] are used to statically schedule TT frames according to the application-specific requirements for the worst-case e2e latency. The other is *Time-Sensitive Networking* (TSN) [12], defined and refined by the IEEE 802.1 TSN Task Group as an extension of the IEEE 802.3 Ethernet for real-time transmission since 2012. It employs IEEE 802.1AS [13] (based on IEEE 1588 [14], a precision clock synchronization protocol) to synchronize all devices participating in real-time communication. Traffic is labeled with different priorities and scheduled to meet different time-critical requirements in the mixed transmission, which is standardized as IEEE 802.1Qbv [15]. 802.1Qbv uses time-aware transmission gates to separate transmission queues for different traffic classes. The transmission gates are opened and closed at specific times according to a time-based circular scheduler. These TT schedulers [8]–[11] are compatible with the time-aware transmission and have already been applied to TSN in [16]–[18].

However, scheduling TT frames by assigning them precise transmission time instants is a bin-packing problem, which is known to be NP-complete. Thus, TT schedulers [8]–[11], [16]–[18] usually search for application-specific worst-case e2e latency constraints as deadlines so as to reduce the time to solve and enhance schedulability. Furthermore, under this scheduling policy, the TT frames cannot be sent sooner than their scheduled sending time even when the network is idle. For example, given a frame of 64 bytes under fast Ethernet (100 Mbps), the application-specified e2e latency $200\mu s$, and the path from A to F illustrated in Fig. 1, a feasible solution for the scheduled sending times may be $0ns$ for end-device A, $80,000ns$ for switch D, and $180,000ns$ for switch E. This solution meets the latency requirement but needs about $\approx 180\mu s$ to deliver the frame. In fact, using BE delivery, the forwarding latency for the frame, defined as the latency from the first bit received by the switch to the first bit sent out by the switch, is $7.92\mu s$ in the absence of congestion in our fast Ethernet switch. Therefore, the e2e latency is about $20\mu s$ from A to F without congestion. The latency is 10x shorter than

Zonghui Li, Wenlin Zhu are with the Beijing Key Laboratory of Transportation Data Analysis and Mining, School of Computer and Information Technology, Beijing Jiaotong University, Beijing, China, 100044. Zonghui Li is the corresponding author. E-mail: zonghui.lee@gmail.com, zhuwenlin@bjtu.edu.cn.

Kang G. Shin is with the Department of Electrical Engineering and Computer Science, University of Michigan, Ann Arbor, MI 48109-2121, USA. E-mail: kgshin@umich.edu.

Hai Wan is with the Software School, Tsinghua University, Beijing, China, 100084. E-mail: wanhai@tsinghua.edu.cn.

Xiaoyu Song is in the Department of Electrical and Computer Engineering, Portland State University, Portland, OR. E-mail: songx@pdx.edu.

Dong Yang, Bo Ai are with the School of Electronic and Information Engineering, Beijing Jiaotong University, Beijing, China, 100044. E-mail: dyang@bjtu.edu.cn, boai@bjtu.edu.cn.

that of TT transmission. As a result, TT frames are delivered much slower than non-real-time BE frames! That is, there exists a big latency gap between TT transmission and BE transmission, making us wonder whether it is good enough for time-critical applications to only guarantee their deadlines by the TT transmission mode.

In the context of Industry 4.0 [3], [19], the timely delivery of control frames by industrial networks is vital to different control steps in industrial distributed systems. The faster the frames are delivered, the closer these control steps are in order to achieve shorter response time and higher efficiency. For example, fast delivery for emergency braking in high-speed trains can gain more time to avoid accidents. Another example is healthcare monitoring, especially for life-critical heart condition. Besides meeting deadlines, fast delivery of such monitoring messages will enable a more timely and efficient response to health problems. So, networks need to reduce delay beyond what e2e deadlines require. However, TT transmission satisfies the e2e deadlines of time-critical frames by scheduling their precise sending instants in switches that could hamper their fast delivery. On the other hand, BE frames are forwarded using strategies like strict priority (SP), weighted round robin priority (WRR), credit-based traffic shaping (CBS) [20]–[22] and asynchronous traffic shaping (ATS) [23], [24], so as to ensure their delivery as soon as possible. Nonetheless, such transmission strategies do not guarantee the e2e deadlines and may even lead to their loss due to queuing, rerouting, congestion, etc. So, the BE transmission is unacceptable for industrial control applications, and moreover, TT transmission and BE delivery are incompatible to each other.

To exploit both BE and TT transmissions, we propose a synergistic switch architecture (SWA) to forward TT frames as soon as possible — without waiting until their scheduled sending times — and meet their e2e latency constraints; our preliminary results were reported in [25]. The architecture forwards the cloned TT frames with BE delivery to speed up the transmission of TT frames. That is, a TT frame and its copy are forwarded with TT and BE strategies, respectively. Whichever of the two copies arrives at the end-device first is delivered to the receiver application and the other copy is discarded. As a result, the e2e latency of the delivered copy is likely to be shorter than that of the TT frame. Furthermore, to handle the possible loss of frame copies, cloning happens at each switch along the routing path of a TT frame. By comparing the strictly-increasing sequence number of TT frames, the SWA guarantees the transmission of only one cloned copy of each TT frame. Therefore, the bandwidth cost for the BE transmission of cloned copies is equal to the cost bandwidth of TT frames.

In fact, the SWA only uses the unused bandwidth of BE transmission because it opportunistically delivers these copies. The congestion, if happens, lets the copies be dropped. Once the copies have an opportunity to be transmitted, they will be delivered again. Such an opportunism allows the SWA to dynamically improve the e2e latency of TT frames and adapts to the changes of the available BE bandwidth. Moreover, the bandwidth cost of TT frames for industrial control

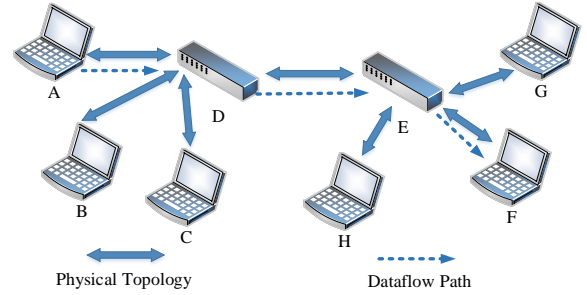


Fig. 1. Example of a TT network with 6 terminal systems and 2 switches.

systems is usually low. For example, the multifunction vehicle bus (MVB) [26] for a train communication network has a bandwidth of up to 1.5 Mbps. The controller area network (CAN) [27] for the automotive industry has a bandwidth of up to 1 Mbps. Consequently, the copies only consume a small portion of bandwidth, making SWA cost-efficient. In addition, according to statistics [28], in Ethernet, packets using Type of Service and Differentiated Service Code Point account for 18% of the enterprise network traffic. So, the copies set as high priority traffic will always have a high probability to improve the transmission of TT frames with BE delivery. Finally, to control the *jitter* (defined as the difference of the maximum and minimum latency) of a delivered frame, we extend the preliminary architecture in [25] to support a configured jitter by holding the frame until the jitter is less than a configured range.

We have implemented the proposed architecture in our industrial TT switches with Xilinx FPGA Virtex-7 XC7VX485T. Four test scenarios are presented to demonstrate the improvement and controllable jitter of the e2e latency of TT frames against the state-of-the-art TT transmission [8], [29]. This paper makes the following main contributions:

- Proposal of a synergistic switch architecture (SWA) and its five forwarding steps as well as their respective algorithms covering the entire forwarding process of the copies of TT frames from ingress into a switch to egress from the switch.
- Four properties of the SWA that dynamically improve the e2e latency of TT frames by opportunistically exploiting BE transmission.
- Extension of the architecture to support controllable jitters by holding those delivered frames until the jitters fall in their configured ranges.
- Implementation of the SWA in our FPGA-based industrial TT switches and demonstration of four test scenarios to validate its dynamical latency improvement and controllable jitter for TT frames compared to the current TT transmission.

The rest of the paper is organized as follows. Section II discusses related work and describes the SWA's novelty. Section III describes the background for TT transmission and the problems of designing such a SWA. Section IV details the design, algorithms and properties of the SWA. Section V evaluates the switch architecture for four test scenarios and

compares it with the current TT transmission. Finally, Section VI concludes the paper.

II. RELATED WORK

Although time-triggered networks integrate TT and BE transmissions, the two types of transmission are still independent in the switch architecture for transmission of their respective frames. 802.1Qbv [15] employs a gate control list at the scheduled sending time instants to separate TT frames from BE frames, and uses guard-band or preemption strategies [30] to reduce the effect of BE frames on TT frames. [29], [31], [32] follow the switching scheme of 802.1Qbv. [31] proposes a template-based TSN-builder to customize TSN switches according to an application-dependent resource abstract. [32] co-designs FIFO scheduling constraints with hardware sequence checking of TT frames to improve usage rate of queues. Furthermore, [29] presents a memory-switch architecture and shared-memory scheduling constraints to make all ports share on-chip memory. To the best of our knowledge, the proposed SWA is the first cooperative TT and BE transmissions. It uses BE transmission to collaboratively deliver clone copies of TT frames to improve the e2e latency of TT transmission. It is different from the multipath redundancy of 802.1Qca [33] which uses multiple redundant paths for TT frames and all paths are used to transmit TT frames with TT transmission. [34] presents a multipath redundant scheduler for TT transmission.

TT transmission depends on TT scheduling [8]–[11], [16]–[18] to plan the precise sending instants of TT frames in each of end-devices and switches according to the application-specific e2e latency requirements, especially for industrial control. Scheduling results are transformed to schedule tables as the configuration of switches. Based on schedule tables, switches send TT frames at their precise sending instants for real-time control. [8] first formalizes TT scheduling by linearizing constraints such as e2e delay, free contention, and limited buffers, and then uses a satisfiability-modulo-theories (SMT) solver [35] to iteratively solve the scheduling problem. [9] tunes the configuration parameters of SMT solvers for enhancing performance. [10], [11] decomposes the scheduling constraints into multiple subsets and solves them incrementally to reduce the solution time. Especially, [16]–[18] linearize the constraints of 802.1Qbv. [17] uses the first-order theory of arrays to directly generate the gate control list of 802.1Qbv. Recently, heuristic strategies [36]–[42] have been proposed to speed up TT scheduling. In addition, BE frames are transmitted in the interval between TT frames. To improve the quality of service (QoS) of BE transmission, [43], [44] use a Tabu Search-based meta-heuristic algorithm to adjust the interval between TT frames. Such an interval adjustment even worsens the e2e latency of TT frames. All these schedulers generate the precise sending instants for TT frames in each device. They prevent the transmission of TT frames as soon as possible since they must wait until their time instants.

Our proposed SWA can in theory improve any scheduler for TT transmission, namely, both previous and future TT schedulers that modify the previous schedulers to minimize the e2e latency of TT frames, since it opportunistically exploits

BE transmission to deliver TT frames as soon as possible. In other words, SWA can improve the e2e latency of TT frames as long as BE transmission is possible.

III. BACKGROUND AND PROBLEM DEFINITION

This section first presents the background for TT transmission, and then details the problems in designing a synergistic switch architecture.

A. Background

1) *Basic terminology and Concepts*: We model the topology of a network as an undirected graph $G(V,E)$, where vertices V represent the end-systems and switches and edges E represent the physical communication links connecting vertices. Fig. 1 shows an example network topology with 8 vertices including 6 end-systems and 2 switches. An ordered tuple $[v_i, v_j], v_i, v_j \in V$ defines a directed “dataflow links” from v_i to v_j . A sequence of dataflow links l_i forms a “dataflow path”. An example of a dataflow path from A to F is depicted by the dotted line in Fig. 1. We formally express a dataflow path p from a sender v_0 to a receiver v_{n+1} by the sequence of its dataflow links:

$$p = [[v_0, v_1], \dots, [v_n, v_{n+1}]],$$

where the dataflow path has n switches (i.e., v_1, v_2, \dots, v_n). Thus, a dataflow path defines a route from a sender to exactly one receiver.

Information between the sender and the receiver is communicated in the form of TT flows that are composed of periodic TT frames according to AS6802. Let F denote the set of TT flows. A flow $f_i \in F$ on a dataflow link $[v_k, v_l], f_i^{[v_k, v_l]}$ is temporally specified by the following quadruple:

$$f_i^{[v_k, v_l]} = \{f_i.\text{period}, f_i^{[v_k, v_l]}.offset, f_i.length, f_i.sequence\}.$$

The period and length of a flow are specified by the underlying application. The flow sequence identifies different TT frames of the same flow in different periods. $f_i^{[v_k, v_l]}.offset$ is the departure time of flow f_i from vertex v_k to vertex v_l and is assigned by TT schedulers.

2) *Time-triggered transmission*: Scheduling results are transformed into schedule tables stored in devices. These devices send flows at the specific times according to schedule tables. For example, the n -th departure time of flow f_i from vertex v_k to v_l is specified by $n * f_i^{[v_k, v_l]}.period + f_i^{[v_k, v_l]}.offset$. However, besides TT frames, TT networks also transmit BE frames. Two typical methods have been used to avoid the conflict with BE frames. One is non-preemptive with a guard band in front of each TT frame transmission (according to the IEEE 802.1 Qbv-2015, Amendment 25: Enhancements for Scheduled Traffic), which assures the BE transmission can be done before transmitting TT frames. The other is preemptive with minimal guard band (according to the IEEE 802.1 Qbv-2016, Amendment 26: Frame Preemption), which minimizes the waiting time of TT frames in case of conflict. So, in TT networks, we assume all flows are sent with no waiting at the time of their departure.

Actually, given no-wait transmission, the processing delay from the departure time $f_i^{[v_k, v_l]}.offset$ to the first bit of flow f_i on the dataflow link $[v_k, v_l]$ is constant, denoted by $pdelay^{[v_k, v_l]}$. We also let $ldelay^{[v_k, v_l]}$ be the link delay on $[v_k, v_l]$, which is measured dynamically by the peer delay mechanism of the IEEE 1588. Hence, the time of arrival at vertex v_l for flow f_i is:

$$f_i^{[v_k, v_l]}.arrival = f_i^{[v_k, v_l]}.offset + pdelay^{[v_k, v_l]} + ldelay^{[v_k, v_l]}.$$

However, TT networks depend on time synchronization whose accuracy, denoted by μ , is defined as the maximum time difference of any two synchronized devices in the network. In theory, the jitter of the arrival time of flow f_i is in the range $[f_i^{[v_k, v_l]}.arrival - \mu, f_i^{[v_k, v_l]}.arrival + \mu]$. In practice, depending on the implementation, the jitter is affected by the processing jitter, queuing policies, etc. Hence, the time of flow f_i arriving at switch v_l is in a time window denoted by the range $[f_i^{[v_k, v_l]}.arrival-start, f_i^{[v_k, v_l]}.arrival-end]$. Assuming the first dataflow link and the last dataflow link of flow f_i are $[v_0, v_1]$ and $[v_n, v_{n+1}]$, respectively, the e2e latency of flow f_i ranges from $f_i^{[v_n, v_{n+1}]}arrival-start - f_i^{[v_0, v_1]}offset$ to $f_i^{[v_n, v_{n+1}]}arrival-end - f_i^{[v_0, v_1]}offset$. The latency jitter is $f_i^{[v_n, v_{n+1}]}arrival-end - f_i^{[v_n, v_{n+1}]}arrival-start$.

B. Problems of Designing A SWA

TT transmission tends to hold frames until their scheduled sending time even when they can be transmitted right away. In contrast, BE transmission delivers frames as soon as possible but its uncertainties in rerouting, congestion, and queuing do not ensure the satisfaction of e2e frame latency requirement. So, designing a SWA must address the uncertainty of BE transmission to improve TT transmission. First, TT transmission is order-preserving due to the scheduled TT frames. However, rerouting may lead to out-of-order frames in BE transmission while it is easy to preserve delivery order with static routing. SWA keeps copies of TT frames along with the same paths as those of TT frames with static routes. Frame loss can also lead to out-of-order delivery if the frame copy of a TT flow at the i -th period is lost due to congestion but the copy at the $(i + 1)$ -th period over-takes the i -th TT frame. SWA employs a sequence-based order-preserving strategy to drop such out-of-order copies and restore the right sequence.

Second, TT transmission guarantees the bounded e2e latency by transmitting TT frames at their scheduled precise sending instants. However, in BE transmission, queuing will delay the forwarding of copies of TT frames. As a result, a longer latency may incur to TT frames. Furthermore, frame loss will result in unreachable copies. SWA ensures that the latency of TT frames is the worst-case e2e latency because either a TT frame or its copy, whichever arrives first at the destination device, will be kept while discarding the other. Moreover, SWA allows frame loss. For example, a switch has frame loss due to congestion but the remaining path from its next switch to the destination is available. The proposed SWA can recover the copy from the next switch to continue improving the remaining latency of TT frames.

Finally, TT transmission guarantees the latency jitter to be in the time window determined by the time synchronized accuracy, the processing jitter of a switch, etc. However, in BE transmission, when a frame is forwarded without congestion in all devices along its path, the frame has the minimum e2e latency. As a result, SWA reduces the lower bound of the e2e latency to the minimum. The jitter of a TT frame is the difference between the minimum latency of its copy and the latency of the TT frame with the worst-case e2e latency in SWA. To combat the negative effects of the jitter, we extend the architecture to support a configurable jitter. The extended architecture makes a tradeoff between the jitter and the latency according to the application requirements. That is, the smaller the jitter, the higher the lower bound of the latency.

IV. SYNERGISTIC SWITCH ARCHITECTURE

The SWA uses BE transmission to enhance the performance of TT transmission. It defines the forwarding paradigm from ingress into a switch to egress from the switch for TT frame copies, as illustrated in Fig. 2. The solid rays indicate data flows (frames) and the dotted rays indicate control flows (table data). The forwarding paradigm contains four tables with dotted rectangles and five processing steps with solid rectangles, which is different from the standard forwarding scheme [29] that does not handle the uncertainty of BE transmission.

A. Forwarding Tables

TT flows are scheduled to have the precise departure times and the scheduled results are transformed into schedule tables in devices. The content of the schedule table [29] is illustrated as Fig. 3(a). *flow-id* and *sequence* identify a unique flow and a unique TT frame of the flow, respectively. The *sequence* also indicates the order of TT frames appearing in a flow. We assume that the sequence number is predictable. That is, given the current sequence number, the expected next sequence number can always be calculated. Furthermore, for simplicity, the expected next is equal to the current plus one. *sequence* is updated based on the forwarding processes of the proposed architecture. *period* is the time interval of a regularly repeating flow. For example, if the period of a flow is 1 *ms*, its frame will be transmitted every 1 *ms*. *length* is the valid payload as bytes of a flow. The valid payload does not contain the cyclic redundancy check (4 bytes), preamble and start frame delimiter (8 bytes), and the shortest inter-frame gap (12 bytes). *input-port* and *output-port* are the input port and the output port, respectively, in a switch according to the dataflow path of a flow. *arrival-start* and *arrival-end* is the time window of the flow arriving at a switch. *offset* is the departure time of a flow from a switch.

Copies of TT frames are transmitted using BE strategies. To ensure that copies follow the same dataflow paths as those of TT frames, they are forwarded according to a static route table which is illustrated in Fig. 3(b). *flow-id* is treated as the index to access the static route table. *length* and *input-port* are used to check a copy frame. Any discordance will lead to drop the copy frame. *output-port* is the forwarding

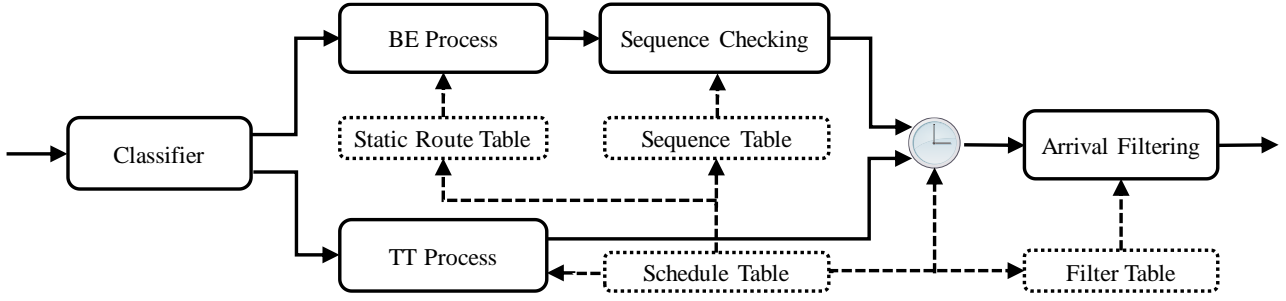


Fig. 2. The synergistic switch architecture. Each solid rectangle means one processing step for the architecture. Each dotted rectangle means one table used by the corresponding processing step. The solid rays indicate data flows (frames). The dotted rays indicate control flows (table data).

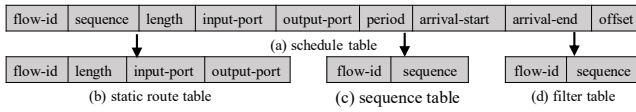


Fig. 3. Tables in the SWA. (a) is the content of the entire schedule table. (b), (c) and (d) are *static-route-table*, *sequence-table* and *filter-table*, respectively, and their initialization sources from *schedule-table*.

port of the copy. To preserve the order of copies in a flow, the sequence numbers of copies are checked with a sequence table illustrated in Fig. 3(c). Finally, to make sure that only one frame, either a TT frame or its copy, is received by the destination device, we drop the later frame and deliver the first arrival frame by a filter table as illustrated in Fig. 3(d), in the output port of the last switch of a dataflow path. Fig. 3 presents the contents of all tables. (b), (c), and (d) are newly added for the proposed architecture and their initialization sources from (a). The updates of data fields in these tables are based on the forwarding processes of the proposed architecture.

B. Forwarding Processes

Fig. 2 shows the overall proposed switch architecture. Following the dataflow in the architecture, five processing steps are performed to handle TT frames and their copies. The *Frame* is the basic data structure for the architecture, which at least contains these data fields, namely *flow-id*, *sequence*, *length*, *input-port*, *arrival-time* and *iscopy*. *arrival-time* is recorded by timestamps when the frame arrivals at a device. *iscopy* equal to true indicates a cloned copy, else a TT frame.

Step 1: Classifier is illustrated in Alg. 1. It classifies the received frames by the data field *iscopy*. If a frame is a copy, then proceed to Step 2 *BE process*. If a frame is a TT frame, the frame is first cloned to generate a new copy and then move to Step 3, *TT process*. Its copy proceeds to Step 2 *BE process*. The cloning happens at each switch.

Step 2: BE process is illustrated in Alg. 2. It searches *static-route-table* by *flow-id* and then checks *length* and *input-port*. If matched, the frame is forwarded to the corresponding output port based on *output-port*. Otherwise, the frame is dropped.

Step 3: TT process is illustrated in Alg. 3. It searches *schedule-table* by *flow-id*. The arrival time, *arrival-time*, of

Algorithm 1: Classifier

Input: FIFO<Frame> frames
Output: FIFO<Frame> TTs, TTcopies

```

1 while !frames.empty() do
2   Frame frame = frames.dequeue();
3   if frame.iscopy then
4     TTcopies.enqueue(frame);
5   end
6   else
7     Frame newframe = copy(frame);
8     newframe.iscopy = true;
9     TTs.enqueue(frame);
10    TTcopies.enqueue(newframe);
11  end
12 end

```

Algorithm 2: BE process

Input: FIFO<Frame> TTcopies
Output: FIFO<Frame>[] TTcopiesbyport

```

1 while !TTcopies.empty() do
2   Frame frame = TTcopies.dequeue(TTcopies);
3   Row row = static-route-table[frame.flow-id];
4   if (row.length == frame.length) and (row.input-port
5     == frame.input-port) then
6     TTcopiesbyport[row.output-port].enqueue(frame);
7   end
8   else
9     drop frame;
10  end

```

the frame must range from *arrival-start* to *arrival-end*. The sequence number, *sequence*, of the frame must be larger than that in *schedule-table*, indicating a new TT frame. *length* and *input-port* are also checked. If any unmatched, the frame is dropped. If all matched, a timer is set to $offset + m * period$ for the m -th TT frame. At that time instant, the sequence number of *schedule-table* is updated and the frame is forwarded to the corresponding output. The sequence numbers of TT frames are

Algorithm 3: TT process

```

Input: FIFO<Frame> TTs
Output: FIFO<Frame>[] framesbyport
1 while !TTs.empty() do
2   Frame frame = TTs.dequeue();
3   Row row = schedule-table[frame.flow-id];
4   if (frame.arrival-time ≤ row.arrival-end) and
      (frame.arrival-time ≥ row.arrival-start) and
      (row.length == frame.length) and (row.input-port
      == frame.input-port) and (frame.sequence >
      row.sequence) then
5     SetTimer(row.offset) {
6       row.sequence = frame.sequence;
7       framesbyport[row.output-port].enqueue(frame);
8       Row strow = sequence-table[frame.flow-id];
9       if frame.sequence > strow.sequence then
10        | strow.sequence = frame.sequence;
11      end
12    };
13  end
14  else
15    | drop frame;
16  end
17 end

```

used to restore the sequence numbers in *sequence-table* for the cloned copies due to the uncertainties of the BE transmission, such as congestion and queuing. When the sequence number of the TT frame is larger than that in *sequence-table*, it indicates that the cloned copies fall behind the TT frame due to congestion and queuing, and thus the sequence number in *sequence-table* is updated so as to drop those copies falling behind in Step 4, *sequence checking*. Although multiple timers may be set, these operations are still conflict-free due to the TT scheduling that ensures different TT frames are not forwarded to the same port at the same time.

Step 4: Sequence checking is illustrated in Alg. 4. It searches *sequence-table* by *flow-id* and checks if the current sequence number of the frame *frame.sequence* is equal to the expected sequence number *row.sequence + 1*. If equal, the sequence number in *sequence-table* is updated and the frame is passed to the corresponding output port, else the frame is dropped. Such a checking for sequence numbers ensures that cloned copies strictly follow the sequence number one-by-one, and thus is order-preserving. Any uncertainty such as surpassing or falling behind will lead to dropping of copies in the sequence checking. If such an uncertainty happens, the sequence numbers in *sequence-table* are restored by Step 3, *TT process*. TT copies sent as BE frames do not create any conflict with TT frames due to the use of a guard band for TT transmission, and thus the updates of sequence numbers by this step and Step 3, *TT process*, do not have any conflict.

Step 5: Arrival filtering is illustrated in Alg. 5. It searches *filter-table* by *flow-id* and checks the sequence number of the frame. If the sequence number is larger than that in *filter-table*, the frame is delivered to the corresponding output port

Algorithm 4: sequence checking

```

Input: FIFO<Frame>[] TTcopiesbyport
Output: FIFO<Frame>[] framesbyport
1 for  $i = 0; i < TTcopiesbyport.num; i++$  do
2   while !TTcopiesbyport[i].empty() do
3     Frame frame = TTcopiesbyport[i].dequeue();
4     Row row = sequence-table[frame.flow-id];
5     if frame.sequence == row.sequence + 1 then
6       | row.sequence = frame.sequence;
7       | framesbyport[i].enqueue(frame);
8     end
9     else
10    | drop frame;
11    end
12  end
13 end

```

Algorithm 5: Arrival Filtering

```

Input: FIFO<Frame>[] framesbyport
Output: FIFO<Frame>[] deliveredframes
1 for  $i = 0; i \leq framesbyport.num; i++$  do
2   while !framesbyport[i].empty() do
3     Frame frame = framesbyport[i].dequeue();
4     Row row = filter-table[frame.flow-id];
5     if frame.sequence > row.sequence then
6       | row.sequence = frame.sequence;
7       | deliveredframes[i].enqueue(frame);
8     end
9     else
10    | drop frame;
11    end
12  end
13 end

```

and updates the sequence number in *filter-table*. Otherwise, the frame is dropped. This step performs filtering the later-arriving frames to ensure only the earlier piece, namely either a TT frame or its copy, is delivered. It is usually enabled at the latest switch that is directly connected to the end-device in a route. Depending on demands, the data field *iscopy* may be recovered to false so that the end-device treats it as a TT frame. If this step is disabled, the end-device may receive both a TT frame and its copy without the arrival filtering.

In addition, the processing steps, namely, Steps 3–5, depend on the incremental sequence numbers. So, it is necessary to ensure the initial value of a sequence number in tables is equal to the minimal value like 0. When devices are initialized, or configurations are updated, the sequence number should be reset.

C. Guaranteed Properties

To improve the e2e latency of TT transmission via BE transmission, the underlying architecture should have the following four properties:

- *Preserving Order*: TT transmission is typically for industrial control data whose sequence is rigidly constrained by industrial requirements. The order of TT frames is met by scheduling their transmission at precise instants. So, the architecture should not alter the order of transmitting TT frames in spite of the uncertainty of BE transmission.
- *Self-Recovery*: The queuing and frame loss of BE transmission due to congestion are usually short-lived and partial. So, the architecture should recover the transmission when the congestion disappears.
- *Improvement*: The architecture should improve the e2e latency of TT frames.
- *Cost-Efficiency*: The overhead of the architecture should be low.

The proposed SWA provides four salient properties as follows.

Property 1 (Preserving Order of Transmitting TT Frames). *Different TT frames in a flow from the origin device are received by the end-devices in the same order the origin device sent.*

Proof. Assuming the architecture is not order-preserving, the order of transmitting TT frames is not the same as the order of their reception. Let f_i denote the TT frame with the sequence number i . All transmitted frames have a strictly increasing sequence numbers, i.e., f_i is sent earlier than $f_j \forall i < j$. Due to the difference between the sent and the received order, whatever surpassing or falling behind, there exist two contiguously received frames, f_p and f_q , $p > q$, but f_p is received before f_q . Moreover, since f_p and f_q belong to the same flow with different sequence numbers, they travel on the same static route and data flow path.

If both f_p and f_q are copies, upon receipt of f_p by an end-device, the sequence numbers of *sequence-tables* on the data flow path are all updated to p . Checking $frame.sequence == row.sequence + 1$ will lead to dropping of f_q .

If f_p and f_q are both TT frames, after f_p is received by an end-device, the sequence numbers of *schedule-tables* along with the data flow path are all updated to p . Checking with $frame.sequence > row.sequence$ will lead to dropping of f_q .

If either f_p or f_q is a copy and the other is a TT frame, after an end-device receives f_p , the sequence number of *filter table* in the data flow path is updated to p . Checking with $frame.sequence > row.sequence$ will lead to dropping of f_q .

In all of the above cases, f_q will be dropped, a contradiction since f_q is received. So, the synergistic architecture is order-preserving. \square

Although bandwidths are reserved at specific sending instants for TT frames via their scheduling and TT frames do not have conflict with BE frames under the guard-band strategy, they may still be dropped since the network environment is dynamic and complex such as link or switch failures. So, the condition $frame.sequence > row.sequence$ is checked in *TT process* and *arrival filtering* to recover the transmission of TT frames whenever a new TT frame arrives. However,

the *sequence checking* step checks sequence numbers with $frame.sequence == row.sequence + 1$ because it is used for the transmission of copies of TT frames with the uncertainty of BE transmission. For example, considering the case when a copy with the sequence number m is dropped at a switch v due to congestion while the next copy with sequence number $m + 1$ overtakes the TT frame with sequence number m and also arrives at v , if *sequence checking* also uses $frame.sequence > row.sequence$, the copy with sequence number $m + 1$ will be forwarded. As a result, the sequence number in *filter-table* is updated to $m + 1$, and thus the TT frame with sequence number m will be filtered out. So, checking $frame.sequence > row.sequence$ in *sequence checking* will lead to dropping of TT frames, which is unexpected because BE transmissions are introduced to make TT transmissions as soon as possible, and thus should not hurt the transmission of TT frames.

Hence, we use the checking of $frame.sequence == row.sequence + 1$ in *sequence checking*. But, it may drop all the following copies if a copy is dropped. To deal with such a situation and recover the transmission of the copies, we first establish the following lemma.

Lemma 1. *For a flow $f \in F$, $p = [[v_0, v_1], \dots, [v_n, v_{n+1}]]$ is a dataflow path of f , the constant C is the minimum forwarding time in a single switch. If $f^{[v_n, v_{n+1}]} .offset - f^{[v_0, v_1]} .offset < f.period + n * C$, we have $f^{[v_k, v_{k+1}]} .offset - f^{[v_0, v_1]} .offset < f.period + k * C$ for all dataflow links, $[v_k, v_{k+1}] \in p, 0 \leq k \leq n$.*

Proof. Since C is the minimum forwarding time in a single switch. We have

$$(n - k) * C \leq f^{[v_n, v_{n+1}]} .offset - f^{[v_k, v_{k+1}]} .offset.$$

By $f^{[v_n, v_{n+1}]} .offset - f^{[v_0, v_1]} .offset = (f^{[v_n, v_{n+1}]} .offset - f^{[v_k, v_{k+1}]} .offset) + (f^{[v_k, v_{k+1}]} .offset - f^{[v_0, v_1]} .offset)$, we have

$$(n - k) * C + (f^{[v_k, v_{k+1}]} .offset - f^{[v_0, v_1]} .offset) \leq f^{[v_n, v_{n+1}]} .offset - f^{[v_0, v_1]} .offset.$$

Since $f^{[v_n, v_{n+1}]} .offset - f^{[v_0, v_1]} .offset < f.period + n * C$, we have

$$(n - k) * C + (f^{[v_k, v_{k+1}]} .offset - f^{[v_0, v_1]} .offset) < f.period + n * C, \text{ and thus}$$

$$f^{[v_k, v_{k+1}]} .offset - f^{[v_0, v_1]} .offset < f.period + k * C. \quad \square$$

the minimum forwarding time in a single switch, C , can be achieved by testing, or by its product specification. $\forall f \in F$, we constrain the e2e latency as:

$$f^{[v_n, v_{n+1}]} .offset - f^{[v_0, v_1]} .offset < \min\{period + n * C, latency\}. \quad (1)$$

Finally, we use previous algorithms to schedule these flows. The dropped copies in those scheduled flows will not affect the transmission of the following copies. The formal self-recovery property is given as:

Property 2 (Self-Recovery). *If a flow $f \in F$ satisfies Eq. (1), then it is self-recoverable, i.e., if its copy with sequence number m is dropped, then the transmission of the next copy with sequence number $m + 1$ will not be affected.*

Proof. Suppose the transmission of the next copy is affected by the dropping of the copy with sequence number m and let v_i denote the switch where the copy is dropped. Since the next copy is affected, it is dropped as a result of checking $frame.sequence == row.sequence + 1$ in *sequence checking*. That is, the TT frame with m arrives at v_i not earlier than the next copy with $m+1$, else the TT frame with m will update the sequence number in *sequence-table* to m , and thus the next copy will not be dropped. So, the latency of the TT frame with m from v_0 to v_i is not smaller than the sum of *period* and the forwarding time of the next copy with $m+1$ from v_0 to v_i . Thus, $f^{[v_i, v_{i+1}]} .offset - f^{[v_0, v_1]} .offset \geq f.period + i * C$. But, the flow f satisfies Equation 1. So, by Lemma 1, $f^{[v_i, v_{i+1}]} .offset - f^{[v_0, v_1]} .offset < f.period + i * C$, a contradiction. Thus, the transmission of the next copy with $m+1$ will not be affected. \square

Property 3 (Dynamic Improvement). *The synergistic architecture makes a dynamic improvement of the e2e latency of TT frames.*

The synergistic architecture makes dynamic improvements in the following three aspects.

- 1) The copy of each TT frame is independently transmitted as soon as possible according to the current network load. So, different copies, even in the same flow, usually have different e2e latencies.
- 2) If a copy is dropped at switch v_i , the latency of the remaining path from v_{i+1} to the end-device will be improved by a new copy starting at switch v_{i+1} because SWA attempts to create a new copy at each switch on the flow's path.
- 3) The latency of TT frames is an upper bound of the e2e latency because the *arrival filtering* selects the first arrived frame, namely, either a TT frame or its copy as the final delivery and ignores the others.

Property 4 (Cost-Efficiency). *For each TT frame, no more than one copy of the TT frame is transmitted simultaneously in the whole network.*

Proof. Since the strict checking of $frame.sequence == row.sequence + 1$ in *sequence checking*, after a copy of a TT frame is transmitted, *row.sequence* will be updated to $row.sequence = frame.sequence$ by Alg. 4. As a result, the other copies of the same TT frame will all be dropped as a result of checking $frame.sequence == row.sequence + 1$. Since *sequence checking* happens at each switch, although each switch tries to copy a TT frame, other copies will be dropped by the switches that generated them after one copy is transmitted. So, in the whole network, no more than one copy of the TT frame is transmitted simultaneously. \square

The above four properties enable the synergistic architecture to opportunistically exploit BE transmissions to dynamically improve the e2e latency of TT frames because they handle the uncertainty of BE transmissions and make the architecture cost-efficient.

D. Extension for Controllable Jitter

Although the SWA optimizes the e2e latency of TT frames, it increases the latency jitter of TT transmissions. In general, given a flow f along with a dataflow path $p = [[v_0, v_1], \dots, [v_n, v_{n+1}]]$, the maximum jitter based on SWA is $f^{[v_n, v_{n+1}]} .arrival-end - n * C$ in theory where C is the minimum forwarding time in a single switch. However, the jitter of TT transmission is $f^{[v_n, v_{n+1}]} .arrival-end - f^{[v_n, v_{n+1}]} .arrival-start$. To limit the jitter, we add a new data field *jitter* into the filter table *filter table* and follow a simple holding strategy to control the jitter. That is, when the flow f arrives before $f^{[v_n, v_{n+1}]} .offset - jitter$, the switch v_n holds it until $f^{[v_n, v_{n+1}]} .offset - jitter$; else the switch delivers the flow immediately. Such a strategy of holding frames controls jitter according to the application requirement by configuring the data field *jitter*. In general, the configurable range of the jitter of flow f is $[0, f.period]$ because the jitter larger than the period will lead to no frame or multiple frames in a period, which is unacceptable for industrial real-time control applications [45]. So, to tolerate such unacceptable configurations, i.e., $jitter \notin [0, f.period]$, we assume that $jitter < 0$ is to minimize the jitter, i.e., dropping all copies and delivering TT frames only, and $jitter > f.period$ represents no constraint on jitter.

However, holding frames until the jitter falls in a configured range fails their original timely transmission. As a result, the held frames may conflict TT frames, copies, and other BE frames. Such conflicts should be properly handled if the extension for controlled jitter is implemented. First, the held frames are copies of TT frames rather than TT frames themselves since the e2e latencies of TT frames are the worst-case values, and thus TT frames need not be held. Second, since the held copies are delivered at the specified sending instants according to the configured jitter, which is akin to TT transmission, the conflict resolutions used by TT transmission can also be applied to handle the conflicts between the held copies and other BE frames. For simplicity, it is even not necessary to handle the conflicts between the held copies and other BE frames because if other BE frames are casually transmitted at the specified sending instants of the held copies, the transmission of copies simply waits sent until the transmission of BE frames is completed. In the worst case, a cloned copy of a TT frame will wait until the transmission time instant of the TT frame. As a result, such a wait yield a smaller jitter. Finally, we provide a resolution to the conflicts between the held copies and other copies, TT frames by constraining the configurable range of a jitter. We define a safe-jitter range such that if the jitter is configured in the range, there will be no conflict between the held copies and other copies, TT frames. Theorem 1 provides the safe-jitter range of each TT flow.

Theorem 1 (Safe Jitter Range). *Let F be the set of all flows having the same output port and N be the number of flows in F . $\forall f_i \in F, 0 \leq i < N$, let $jitter_i$ denote the jitter configuration of f_i . g_{ij} is the minimum gap of the departure time of f_j before the departure time of f_i . Especially, when $j = i$, g_{ii} is $f_i.period$, indicating that the minimum gap of two TT frames of f_i is the period of f_i . C_i is the transmission time of f_i*

under a given bandwidth.¹ So, the safe range of jitter_i is:

$$0 \leq \text{jitter}_i \leq \min\{g_{ij} - C_j \mid 0 \leq j \leq N - 1\}. \quad (2)$$

Proof. First, TT frames are conflict-free as a result of scheduling their transmission. So, given $\forall f_i, f_j \in F, 0 \leq i, j < N$, the transmission of f_j can always finish before the departure time of f_i . That is, $g_{ij} - C_j \geq 0$. Therefore, $\min\{g_{ij} - C_j \mid 0 \leq j \leq N - 1\} \geq 0$.

Second, assuming $g_{ij} > f_i.\text{period}$, we set $g'_{ij} = g_{ij} - f_i.\text{period}$. Thus, g'_{ij} is another gap of the departure time of f_j prior to the departure time of f_i and $g'_{ij} < g_{ij}$, which is a contradiction since g_{ij} is the minimum gap. So, $g_{ij} \leq f_i.\text{period}$. Especially, if $g_{ij} == f_i.\text{period}$ is established, then f_i and f_j are the same flow. Otherwise, f_i and f_j are different flows. Since $g_{ij} == f_i.\text{period}$, another frame of f_i is transmitted at the gap g_{ij} prior to the departure time of f_i . At the same time, a frame of f_j is also transmitted at the gap g_{ij} prior to the departure time of f_i according to the definition of g_{ij} . So, a conflict between f_i and f_j occurs, which is a contradiction since TT frames are conflict-free. Furthermore, since $C_j > 0$, we have that $\min\{g_{ij} - C_j \mid 0 \leq j \leq N - 1\} < f_i.\text{period}$.

Third, given $\forall f_i, f_j \in F, 0 \leq i, j < N$, since $0 \leq \text{jitter}_i \leq \min\{g_{ij} - C_j \mid 0 \leq j \leq N - 1\}$, we have that $0 \leq \text{jitter}_i \leq g_{ij} - C_j$. A held copy of f_i will be transmitted at the gap jitter_i prior to the departure time of flow f_i . So, the held copy will be transmitted after or at the gap $g_{ij} - C_j$ prior to the departure time of flow f_i . Thus, its transmission time does not overlap with that of TT frames of f_j . Hence, the held copy of f_i has no conflict with TT frames of f_j . Since f_i and f_j are generic, the held copies have no conflicts with TT frames under $0 \leq \text{jitter}_i \leq \min\{g_{ij} - C_j \mid 0 \leq j \leq N - 1\}$.

Finally, given $\forall f_i, f_j \in F, 0 \leq i, j < N$, tc_{ik} is a held copy of the TT frame of the k -th period of f_i and tc_{jl} is a held copy of the TT frame of the l -th period of f_j . Since the configurations, jitter_i and jitter_j , the departure time of the held copy, tc_{ik} is $k * f_i.\text{period} + f_i^{[v_n, v_{n+1}]}.\text{offset} - \text{jitter}_i$ while the departure time of the copy, tc_{jl} is in the range from $l * f_j.\text{period} + f_j^{[v_n, v_{n+1}]}.\text{offset} - \text{jitter}_j$ to $l * f_j.\text{period} + f_j^{[v_n, v_{n+1}]}.\text{offset}$. Assuming tc_{ik} and tc_{jl} have conflicts, their transmission times overlap. So, the departure time of tc_{ik} falls in the range from $l * f_j.\text{period} + f_j^{[v_n, v_{n+1}]}.\text{offset} - \text{jitter}_j$ to $l * f_j.\text{period} + f_j^{[v_n, v_{n+1}]}.\text{offset} + C_j$. That is,

$k * f_i.\text{period} + f_i^{[v_n, v_{n+1}]}.\text{offset} - \text{jitter}_i < l * f_j.\text{period} + f_j^{[v_n, v_{n+1}]}.\text{offset} + C_j$. Since $0 \leq \text{jitter}_i \leq \min\{g_{ij} - C_j \mid 0 \leq j \leq N - 1\}$, we have $\text{jitter}_i \leq g_{ij} - C_j$. Thus, $(k * f_i.\text{period} + f_i^{[v_n, v_{n+1}]}.\text{offset}) - (l * f_j.\text{period} + f_j^{[v_n, v_{n+1}]}.\text{offset}) < g_{ij}$. Setting $g'_{ij} = (k * f_i.\text{period} + f_i^{[v_n, v_{n+1}]}.\text{offset}) - (l * f_j.\text{period} + f_j^{[v_n, v_{n+1}]}.\text{offset})$, so g'_{ij} is another gap of the departure time of flow f_j prior to the departure time of flow f_i and $g'_{ij} < g_{ij}$. According to the definition of g_{ij} , g_{ij} is the minimum gap, which contradicts $g'_{ij} < g_{ij}$. Hence, the held copy tc_{ik} has no

¹For example, given the bandwidth, 100 Mbps, the transmission time per bit is 10 ns.

Algorithm 6: Computation of safe Jitter

Input: Flow $fs[N]$, int $C[N]$
Output: int $uppers[N]$

```

1 for  $i = 0; i < N; i++$  do
2    $uppers[i] = fs[i].\text{period};$ 
3   for  $j = 0; j < N; j++$  do
4      $gap = fs[i].\text{period};$ 
5     for  $k = 0; k < \frac{LCM(fs)}{fs[j].\text{period}}; k++$  do
6        $q = (k * fs[j].\text{period} + fs[j].\text{offset}) -$ 
7          $fs[i].\text{offset};$ 
8       if  $q \geq 0$  then
9          $m = \lfloor \frac{q}{fs[i].\text{period}} \rfloor;$ 
10        if  $(m + 1) * fs[i].\text{period} - q < gap$  then
11           $gap = (m + 1) * fs[i].\text{period} - q;$ 
12        end
13      end
14    else
15       $k = \lfloor \frac{(fs[i].\text{offset} - fs[j].\text{offset})}{fs[j].\text{period}} \rfloor;$ 
16      if  $fs[i].\text{offset} - (k * fs[j].\text{period} +$ 
17         $fs[j].\text{offset}) < gap$  then
18         $gap = fs[i].\text{offset} - (k * fs[j].\text{period}$ 
19           $+ fs[j].\text{offset});$ 
20        end
21      end
22    end
23  end
24 end
```

conflicts with the copy tc_{jl} . Since the generality of tc_{ik} and tc_{jl} , the held copies will not conflict with other copies under $0 \leq \text{jitter}_i \leq \min\{g_{ij} - C_j \mid 0 \leq j \leq N - 1\}$.

Given the jitter configuration jitter_i of each flow f_i satisfies $0 \leq \text{jitter}_i \leq \min\{g_{ij} - C_j \mid 0 \leq j \leq N - 1\}$, the held copies have no conflicts with TT frames and other copies. \square

According to the proof of Theorem 1, jitter_i that satisfies $0 \leq \text{jitter}_i \leq \min\{g_{ij} - C_j \mid 0 \leq j \leq N - 1\}$ is also in $[0, f_i.\text{period}]$. So, Theorem 1 constrains the configuration range of jitter of each flow and ensures that the held copies have no conflicts with TT frames and other copies. Algorithm 6 treats the scheduled flows fs and their transmission time C as input and outputs the upper bound of the safe-jitter range of each flow, denoted by $uppers$, according to Theorem 1. N is the number of flows. $LCM(fs)$ denotes the least common multiple of these scheduled flows fs .

V. EVALUATION RESULTS AND ANALYSIS

To demonstrate the advantages of SWA, we compare it with the state-of-the-art TT transmission that uses the typical scheduler [8] to schedule TT frames and uses FPGA-based TT switches [29] to transmit these frames. Based on the TT switches, we implement the proposed SWA in our TT

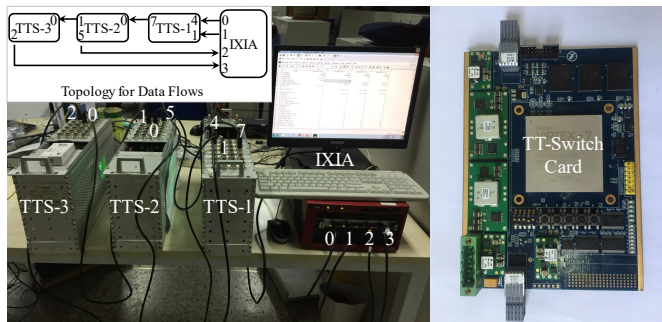


Fig. 4. The experiment platform for the synergetic switch architecture. The IXIA is a standard tester. The TTS-1, TTS-2 and TTS-3 are our time-triggered (TT) switches. The TT-Switch Card is our switch card installed in TTS-1, TTS-2 and TTS-3. The digitals are ports. The rays are links and constitute the topology for data flows.

switches illustrated in Fig. 4 with the Xilinx FPGA Virtex-7 XC7VX485T to demonstrate the practicability of SWA. Our TT switches have 24 fast-Ethernet (100 Mbps) ports. Fig. 4 shows the experiment platform including three TT switches and a standard tester. We designed four scenarios for comparison as follows.

- **Scenario One (Latency Improvement):** We show that the copies of TT frames can always improve the e2e latency of TT frames in spite of the disturbance of other BE data. So, we assign copies a higher priority than that of the other BE data and compare the e2e latency of SWA with that of the previous TT transmission.
- **Scenario Two (Upper Bounds):** We demonstrate that the e2e latency of TT frames is the upper bound of the proposed architecture in the presence of the uncertainty of BE transmission. So, we assign copies of TT frames the same priority as the other BE data. We adjust the bandwidth of the other BE data to queue or even drop copies, and compare the e2e latency of SWA with that of the previous TT transmission.
- **Scenario Three (Self-recovery):** We demonstrate SWA's self recovery by forcing BE transmission congestion to happen. In such a case, some copies of TT frames will be queued or even dropped while others that are delivered faster than TT frames, thus improving TT transmission according to the self-recovery property. So, we assign copies of TT frames the same priority as the other BE data, and adjust BE bandwidth to queue or even drop copies. Furthermore, we let the queuing and loss only happen in some switches to demonstrate that the other congestion-free switches can still improve latency of TT transmission. We present the dynamic improvement in self-recovery scenarios by comparing the e2e latency of SWA with that of the previous TT transmission.
- **Scenario Four (Controllable Jitter):** We show the controlled jitter of our extended architecture by a configurable jitter. So, based on Scenario Two, we configure the jitter of each flow according to Theorem 1, and compare the e2e latency of SWA with that of the previous TT transmission.

TABLE I
THE BASIC INFORMATION OF TT FLOWS, NAMELY *Flow ID*, *Length* AND *Period*.

Flow ID = 1		Flow ID = 2		Flow ID = 3	
Length (Bytes)	Period (ns)	Length (Bytes)	Period (ns)	Length (Bytes)	Period (ns)
128	524288	256	1048576	512	2097152

TABLE II
THE CONFIGURATION OF TT FLOWS PER SWITCH. THE *Flow-id* WHICH IS THE SAME AS THAT IN TABLE. I IS THE SAME FLOW. THE PORT NUMBERS CORRESPOND TO THOSE IN FIG.. 4.

Switch	Flow ID	Input Port	Output Port	Arrival Start(ns)	Arrival End(ns)	Offset (ns)
TTS-1	1	4	7	400	1400	22528
	2	4	7	29072	30072	61440
	3	4	7	67984	68984	120832
TTS-2	1	0	1	22928	23928	45056
	2	0	1	61840	62840	94208
	3	0	1	121232	122232	174080
TTS-3	1	0	2	45456	46456	67584
	2	0	2	94608	95608	126976
	3	0	2	174480	175480	227328

Test Setup: Fig. 4 presents the experimental platform for the SWA. The IXIA is a standard tester supporting IEEE 1588 protocol. TTS-1, TTS-2, TTS-3 are our TT switches. These switches establish time synchronization using a peer-to-peer transport clock strategy defined in the IEEE standard 1588. The numbers and arrowed lines highlight switch ports and links, respectively, which constitute the topology for data flows. We schedule three TT flows of different lengths and periods in the topology by the scheduler [8]. Table I illustrates the basic information of three flows: *flow-id*, *length*, and *period*. Table II provides the configuration of TT flows in each switches. Since Tables *static-route-table*, *sequence-table*, and *filter-table* for copies of TT frames can be directly generated by Tables I and II according to Fig. 3, they are omitted here. The data field *sequence* in these tables is initialized as 0 and updated based on the proposed SWA. All these TT flows are sent from the source, the port 0 of IXIA and are received from the sink, the port 3 of IXIA. The e2e latency of TT frames, defined as the latency from the first bit sent out by the source to the first bit received by the sink, is measured by the standard tester, IXIA. The ports, 1 and 2 of IXIA are used to send and receive other BE data as disturbance traffic, respectively, with the fixed length of 64 bytes and the bandwidth increased by 10 Mbps as step size. We test the e2e latency of TT frames with the previous TT transmission and SWA, respectively, under the four different scenarios as follows.

Scenario One (Latency Improvement): We assign the copies of TT frames higher priority than that of the other

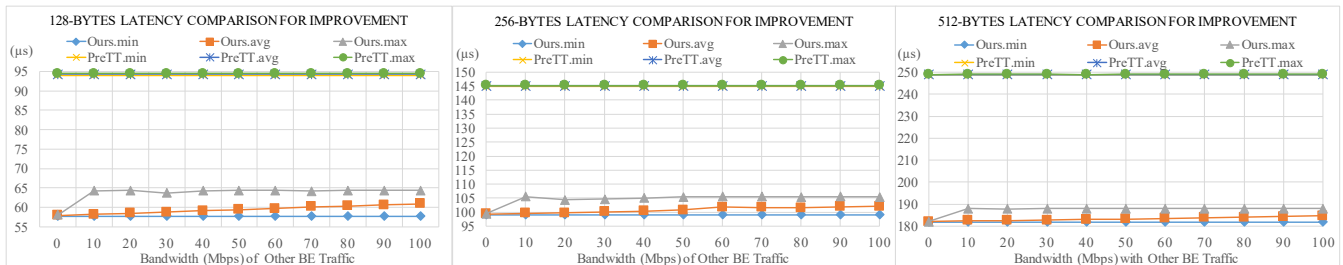


Fig. 5. The e2e latency comparison of SWA and the previous TT transmission, denoted by *PreTT*, under Scenario One. The copies of TT frames of different sizes in SWA have higher priority than that of the other BE traffic which is broadcast and increased by 10 Mbps as step size.

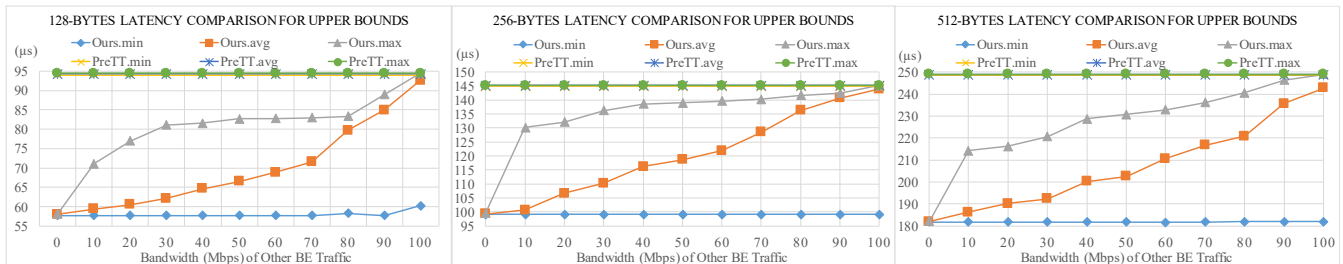


Fig. 6. Comparison of e2e latencies of SWA and the previous TT transmission, denoted by *PreTT*, under Scenario Two. The copies of TT frames of different sizes have the same priority as that of the other BE traffic which is broadcast and increased by 10 Mbps as step size.

BE traffic, and broadcast the BE traffic via port 1 of *IXIA*. First, we disable the functions of SWA by configuring the TT switches to test the e2e latency of TT frames with the previous TT transmission. Fig. 5 plots the latency of TT frames of 128, 256 and 512 bytes. The minimum, average, and maximum latency — *PreTT.min*, *PreTT.avg*, and *PreTT.max*, respectively — are three nearly coincident lines due to the high time-synchronized precision, $500ns$ by IEEE 1588. The latency of TT frames of 128 bytes is about $94.25 \mu s$ and not affected by the broadcast of the BE traffic because of the guard band strategy according to IEEE 802.1 Qbv. Second, we enable the functions of SWA and test the e2e latency of TT frames again. Fig. 5 illustrates the minimum, average, and maximum latency of SWA, namely, *Ours.min*, *Ours.avg*, and *Ours.max*, respectively. Compared to the previous TT transmission, SWA makes a significant improvement in the latency of different frame lengths since the copies are forwarded as soon as possible to enhance the transmission of TT frames. For example, for the 128-bytes frames, the maximum latency of SWA is about $64.34 \mu s$ while the latency of the previous TT transmission is about $94.25 \mu s$. Furthermore, the low-priority BE traffic makes a small impact on the latency of SWA, namely, a $6.5 \mu s$ difference between the maximum and the minimum latency. Even when the bandwidth of the BE traffic reaches 100 Mbps, the high-priority copies are still delivered quickly to improve the latency of TT frames.

Scenario Two (Upper Bounds): The difference from Scenario One is to broadcast the other BE traffic with the same priority as the copies of TT frames. First, we still disable the functions of SWA and test the e2e latency of TT frames with

the previous TT transmission. As a result, Fig. 6 demonstrates the same latency of *PreTT* as that in Fig. 5 due to the scheduled precise sending instants and the guard band strategy. Second, we enable the proposed SWA and test the e2e latency of TT frames again. As illustrated in Fig. 6, the latency changes from the minimum latency up to the latency of the previous TT transmission with different bandwidth of other BE traffic. So, the same priority BE traffic makes a bigger impact on the latency of SWA than that of the low-priority traffic in Scenario One. Furthermore, when the bandwidth of the BE traffic reaches 100 Mbps, the copies start to be dropped due to congestion and our latency reaches up to the latency of the previous TT transmission because SWA selects the first arrival as the final delivery. Hence, the latency of TT frames with the previous TT transmission is an upper bound of SWA's latency.

Scenario Three (Self-recovery): The difference from Scenario Two is to unicast the other BE traffic from port 1 to port 2 of *IXIA*. As a result, the unicast BE traffic will disturb the transmission of copies of TT frames in the link from port 7 of *TTS-1* to port 0 of *TTS-2*, and not affect the link from port 1 of *TTS-2* to port 0 of *TTS-3*. First, we still disable the functions of SWA to test the e2e latency of TT frames with the previous TT transmission. Fig. 7 demonstrates the same latency of *PreTT* as that in Fig. 5 and Fig. 6 because of the scheduled precise sending instants and the guard band strategy. Second, we enable the proposed SWA and test the e2e latency of TT frames again. As illustrated in Fig. 7, the latency of TT frames using SWA remains low with varying unicast BE bandwidth, which is a sharp contrast with the various latencies

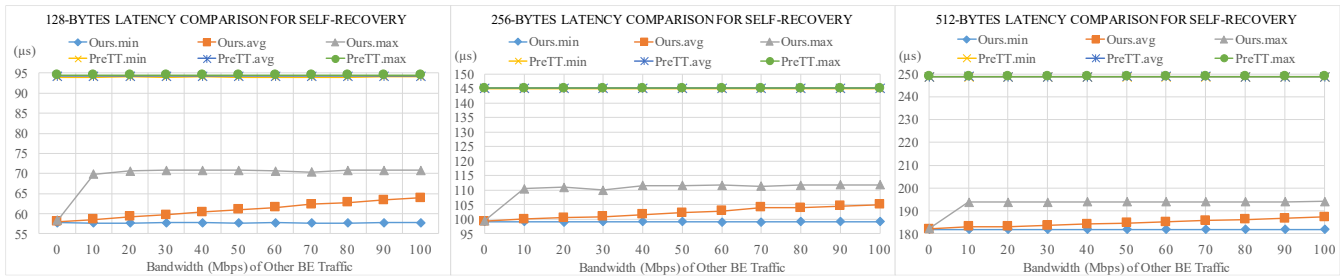


Fig. 7. Comparison of e2e latencies of SWA and the previous TT transmission, denoted by *PreTT*, under Scenario Three. The copies of TT frames of different sizes have the same priority as that of the other BE traffic which is unicast and increased by 10 Mbps as step size.

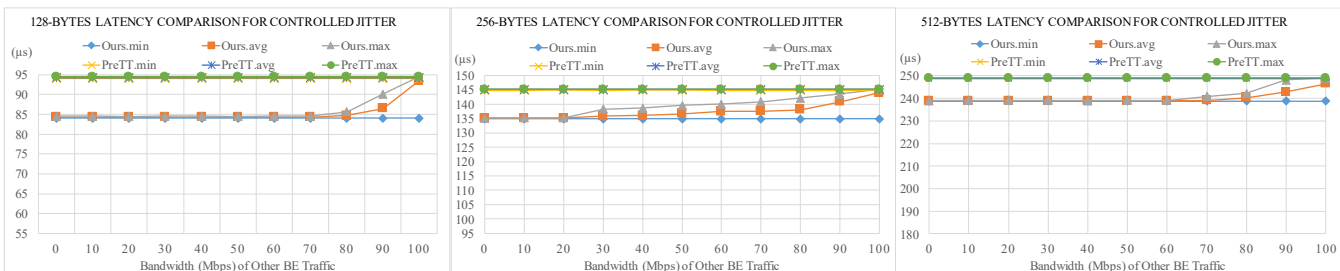


Fig. 8. Comparison of e2e latencies of SWA and the previous TT transmission, denoted by *PreTT*, under Scenario Four. The copies of TT frames of different lengths have the same priority as that of the other BE traffic which is broadcast and increased by 10 Mbps as step size. These copies are transmitted with configured jitters.

in Fig. 6. This is because the BE traffic unicast only impacts the transmission of copies in *TTS-1*. Even if copies are dropped in the presence of 100 Mbps BE traffic, their transmission will recover in the next switch *TTS-2* and continue improving the latency of the remaining path. So, the SWA makes a dynamic and opportunistic improvement of the latency of TT frames.

Scenario Four (Controllable Jitter): Besides the same scenario settings as Scenario Two, we configure the jitters of each flow to constrain the latency jitter of SWA. We compute a safe-jitter range for each flow according to Theorem 1. As a result, $[0, 442496]ns$ for $flow_id = 1$, $[0, 47232]ns$ for $flow_id = 2$, and $[0, 77952]ns$ for $flow_id = 3$. So, we set the jitter configuration, $jitter = 10\mu s$ for all flows and configure the switch *TTS-3*. Fig. 8 illustrates the latency of SWA with the configuration of the controlled jitter, i.e., $jitter = 10\mu s$. Compared to the latency of SWA in Scenario Two illustrated in Fig. 6, the lower bound of the latency is increased and the jitter of TT frames is controlled to be within about $10\mu s$ because the copies are held until the jitter is less than $10\mu s$. For example, for the TT frames of 128 bytes, the lower bound latency is increased to about $84.2\mu s$. When the bandwidth of disturbance traffic is below 70 Mbps, copies are held until their latency reaches the lower bound so that the jitter is no more than $10\mu s$. The jitter configuration constrains the lower latency bound to meet the jitter requirement, suggesting existence of a tradeoff between jitter and latency. That is, the smaller the jitter, the higher the lower latency bound.

In addition, in all scenarios, we carefully compare the

arrival order of TT frames of SWA with that of the previous TT transmission. The proposed SWA is order-perserving. So, these scenarios demonstrate that the proposed SWA tackles the uncertainty of BE transmission and makes a dynamic improvement of the e2e latency of the previous TT transmission. Furthermore, to make a good improvement, it is preferable to assign the copies of TT frames higher priority than that of other BE traffic.

VI. CONCLUSION

TT transmission prevents the delivery of TT frames as soon as possible due to the scheduled precise sending instants, while BE transmission may allow BE frames to be transmitted as soon as possible but may not satisfy the applications' e2e latency requirements. We have proposed a synergistic switch architecture (SWA) by exploiting BE transmission to dynamically and opportunistically enhance TT transmission. Specifically, we have presented the processing steps, requisite table configuration, and algorithms of SWA. We have rigorously investigated the order-preservation, self-recovery, dynamic improvement, and cost-efficiency of the SWA. Furthermore, we have extended the architecture to support the configurable latency jitter by computing the safe jitter range for each TT flow. Finally, we have implemented the proposed SWA in commercial TT switches based on FPGAs and used four scenarios to demonstrate the SWA's capability of dealing with the uncertainty of BE transmission and dynamically improving the e2e latency of TT transmission.

REFERENCES

- [1] S. Vitturi, C. Zunino, and T. Sauter, "Industrial communication systems and their future challenges: Next-generation ethernet, iiot, and 5g," *Proceedings of the IEEE*, vol. 107, no. 6, pp. 944–961, 2019.
- [2] V. Gavriluț, A. Pruski, and M. S. Berger, "Constructive or optimized: An overview of strategies to design networks for time-critical applications," *ACM Computing Surveys*, vol. 55, no. 3, 2022. [Online]. Available: <https://doi.org/10.1145/3501294>
- [3] L. Lo Bello and W. Steiner, "A perspective on IEEE time-sensitive networking for industrial communication and automation systems," *Proceedings of the IEEE*, vol. 107, no. 6, pp. 1094–1120, 2019.
- [4] D. Bruckner, M. Stănică, R. Blair, S. Schriegel, S. Kehrer, M. Seewald, and T. Sauter, "An introduction to opc ua tsn for industrial communication systems," *Proceedings of the IEEE*, vol. 107, no. 6, pp. 1121–1131, 2019.
- [5] A. Minaeva and Z. Hanzálek, "Survey on periodic scheduling for time-triggered hard real-time systems," *ACM Computing Surveys*, vol. 54, no. 1, 2021. [Online]. Available: <https://doi.org/10.1145/3431232>
- [6] Z. Li, H. Wan, Z. Pang, Q. Chen, Y. Deng, X. Zhao, Y. Gao, X. Song, and M. Gu, "An enhanced reconfiguration for deterministic transmission in time-triggered networks," *IEEE/ACM Transactions on Networking*, vol. 27, no. 3, pp. 1124–1137, June 2019.
- [7] "Time-triggered Ethernet," Aerospace standard AS6802, SAE International Group, 11 2011.
- [8] W. Steiner, "An evaluation of SMT-based schedule synthesis for time-triggered multi-hop networks," in *Proceedings of the 2010 31st IEEE Real-Time Systems Symposium*, ser. RTSS '10, 2010, pp. 375–384.
- [9] F. Pozo, G. Rodriguez-Navas, H. Hansson, and W. Steiner, "SMT-based synthesis of TTEthernet schedules: A performance study," in *10th IEEE International Symposium on Industrial Embedded Systems (SIIES)*, June 2015, pp. 1–4.
- [10] F. Pozo, W. Steiner, G. Rodriguez-Navas, and H. Hansson, "A decomposition approach for SMT-based schedule synthesis for time-triggered networks," in *IEEE 20th Conference on Emerging Technologies Factory Automation*, Sept 2015, pp. 1–8.
- [11] S. S. Craciunas and R. S. Oliver, "Combined task-and network-level scheduling for distributed time-triggered systems," *Real-Time Systems*, vol. 52, no. 2, pp. 161–200, 2016.
- [12] N. Finn, "Introduction to time-sensitive networking," *IEEE Communications Standards Magazine*, vol. 2, no. 2, pp. 22–28, 2018.
- [13] "IEEE Standard for local and metropolitan area networks—timing and synchronization for time-sensitive applications," *IEEE Std 802.1AS-2020 (Revision of IEEE Std 802.1AS-2011)*, pp. 1–421, 2020.
- [14] "IEEE Standard for a precision clock synchronization protocol for networked measurement and control systems," *IEEE Std 1588-2008 (Revision of IEEE Std 1588-2002)*, pp. 1–300, 2008.
- [15] "Ieee standard for local and metropolitan area networks – bridges and bridged networks - amendment 25: Enhancements for scheduled traffic," *IEEE Std 802.1Qbv-2015 (Amendment to IEEE Std 802.1Q-2014 as amended by IEEE Std 802.1Qca-2015, IEEE Std 802.1Qcd-2015, and IEEE Std 802.1Q-2014/Cor 1-2015)*, pp. 1–57, 2016.
- [16] S. S. Craciunas, R. S. Oliver, M. Chmelik, and W. Steiner, "Scheduling real-time communication in IEEE 802.1Qbv time sensitive networks," in *Proceedings of the 24th International Conference on Real-Time Networks and Systems*. ACM, 2016, pp. 183–192.
- [17] R. Serna Oliver, S. S. Craciunas, and W. Steiner, "Ieee 802.1qbv gate control list synthesis using array theory encoding," in *2018 IEEE Real-Time and Embedded Technology and Applications Symposium (RTAS)*, 2018, pp. 13–24.
- [18] W. Steiner, S. S. Craciunas, and R. S. Oliver, "Traffic planning for time-sensitive communication," *IEEE Communications Standards Magazine*, vol. 2, no. 2, pp. 42–47, 2018.
- [19] M. Wollschlaeger, T. Sauter, and J. Jasperneite, "The future of industrial communication: Automation networks in the era of the internet of things and industry 4.0," *IEEE Industrial Electronics Magazine*, vol. 11, no. 1, pp. 17–27, 2017.
- [20] "Ieee standard for local and metropolitan area networks - virtual bridged local area networks amendment 12: Forwarding and queuing enhancements for time-sensitive streams," *IEEE Std 802.1Qav-2009 (Amendment to IEEE Std 802.1Q-2005)*, pp. C1–72, 2010.
- [21] L. Zhao, P. Pop, Z. Zheng, and Q. Li, "Timing analysis of avb traffic in tsn networks using network calculus," in *2018 IEEE Real-Time and Embedded Technology and Applications Symposium (RTAS)*, 2018, pp. 25–36.
- [22] L. Zhao, P. Pop, Z. Zheng, H. Daigmore, and M. Boyer, "Latency analysis of multiple classes of avb traffic in tsn with standard credit behavior using network calculus," *IEEE Transactions on Industrial Electronics*, vol. 68, no. 10, pp. 10 291–10 302, 2021.
- [23] "Ieee standard for local and metropolitan area networks—bridges and bridged networks - amendment 34:asynchronous traffic shaping," *IEEE Std 802.1Qcr-2020 (Amendment to IEEE Std 802.1Q-2018 as amended by IEEE Std 802.1Qcp-2018, IEEE Std 802.1Qcc-2018, IEEE Std 802.1Qcy-2019, and IEEE Std 802.1Qcx-2020)*, pp. 1–151, 2020.
- [24] L. Zhao, P. Pop, and S. Steinhorst, "Quantitative performance comparison of various traffic shapers in time-sensitive networking," *IEEE Transactions on Network and Service Management*, vol. 19, no. 3, pp. 2899–2928, 2022.
- [25] Z. Li, H. Wan, B. Zhao, Y. Deng, and M. Gu, "Dynamically optimizing end-to-end latency for time-triggered networks," in *Proceedings of the ACM SIGCOMM 2019 Workshop on Networking for Emerging Applications and Technologies*, ser. NEAT'19. New York, NY, USA: ACM, 2019, pp. 36–42. [Online]. Available: <http://doi.acm.org/10.1145/3341558.3342203>
- [26] "IEC 61375-1: Electric railway equipment-train bus-part 1: Train communication network," International Electrotechnical Commission, April 2007.
- [27] "Road vehicles – controller area network (CAN) – part 2: High-speed medium access unit," ISO Technical Committee, December 2016.
- [28] D. Murray and T. Koziniec, "The state of enterprise network traffic in 2012," in *2012 18th Asia-Pacific Conference on Communications (APCC)*. IEEE, 2012, pp. 179–184.
- [29] Z. Li, H. Wan, Y. Deng, X. Zhao, Y. Gao, X. Song, and M. Gu, "Time-triggered switch-memory-switch architecture for time-sensitive networking switches," *IEEE Transactions on Computer-Aided Design of Integrated Circuits and Systems*, vol. 39, no. 1, pp. 185–198, 2020.
- [30] "IEEE Standard for local and metropolitan area networks – bridges and bridged networks – amendment 26: Frame preemption," *IEEE Std 802.1Qbu-2016 (Amendment to IEEE Std 802.1Q-2014)*, pp. 1–52, 2016.
- [31] J. Yan, W. Quan, X. Yang, W. Fu, Y. Jiang, H. Yang, and Z. Sun, "Tsn-builder: Enabling rapid customization of resource-efficient switches for time-sensitive networking," in *2020 57th ACM/IEEE Design Automation Conference (DAC)*, 2020, pp. 1–6.
- [32] M. Vlk, Z. Hanzálek, K. Brejchová, S. Tang, S. Bhattacharjee, and S. Fu, "Enhancing schedulability and throughput of time-triggered traffic in ieee 802.1qbv time-sensitive networks," *IEEE Transactions on Communications*, vol. 68, no. 11, pp. 7023–7038, 2020.
- [33] "IEEE Standard for local and metropolitan area networks— bridges and bridged networks - amendment 24: Path control and reservation," *IEEE Std 802.1Qca-2015 (Amendment to IEEE Std 802.1Q-2014 as amended by IEEE Std 802.1Qcd-2015 and IEEE Std 802.1Q-2014/Cor 1-2015)*, pp. 1–120, 2016.
- [34] L. Su, H. Wan, Y. Qin, X. Zhao, Y. Gao, X. Song, C. Lu, and M. Gu, "Synthesizing fault-tolerant schedule for time-triggered network without hot backup," *IEEE Transactions on Industrial Electronics*, vol. 66, no. 2, pp. 1345–1355, 2019.
- [35] L. de Moura, B. Dutertre, and N. Shankar, "A tutorial on satisfiability modulo theories," in *Proceedings of the 19th International Conference on Computer Aided Verification*, ser. CAV'07, 2007, pp. 20–36.
- [36] N. G. Nayak, F. Dürr, and K. Rothermel, "Time-sensitive software-defined network (TSSDN) for real-time applications," in *Proceedings of the 24th International Conference on Real-Time Networks and Systems*. ACM, 2016, pp. 193–202.
- [37] Q. Yu, T. Wang, X. Zhao, H. Wang, Y. Gao, C. Lu, and M. Gu, "Fast real-time scheduling for ethernet-based train control networks," in *2018 IEEE Intl Conf on Parallel Distributed Processing with Applications, Ubiquitous Computing Communications, Big Data Cloud Computing, Social Computing Networking, Sustainable Computing Communications (ISPA/IUCC/BDCloud/SocialCom/SustainCom)*, 2018, pp. 533–540.
- [38] N. G. Nayak, F. Dürr, and K. Rothermel, "Incremental flow scheduling and routing in time-sensitive software-defined networks," *IEEE Transactions on Industrial Informatics*, vol. 14, no. 5, pp. 2066–2075, 2018.
- [39] N. Wang, Q. Yu, H. Wan, X. Song, and X. Zhao, "Adaptive scheduling for multicenter time-triggered train communication networks," *IEEE Transactions on Industrial Informatics*, vol. 15, no. 2, pp. 1120–1130, 2019.
- [40] Q. Yu and M. Gu, "Adaptive group routing and scheduling in multicast time-sensitive networks," *IEEE Access*, vol. 8, pp. 37 855–37 865, 2020.
- [41] J. Falk, F. Dürr, and K. Rothermel, "Time-triggered traffic planning for data networks with conflict graphs," in *2020 IEEE Real-Time and Embedded Technology and Applications Symposium (RTAS)*, 2020, pp. 124–136.

- [42] H. Jia, Y. Jiang, C. Zhong, H. Wan, and X. Zhao, "Ttdeep: Time-triggered scheduling for real-time ethernet via deep reinforcement learning," in *2021 IEEE Global Communications Conference (GLOBECOM)*, 2021, pp. 1–6.
- [43] D. Tamas-Selicean, P. Pop, and W. Steiner, "Synthesis of communication schedules for TTEthernet-based mixed-criticality systems," in *Proceedings of the Eighth IEEE/ACM/IFIP International Conference on Hardware/Software Codesign and System Synthesis*, ser. CODES+ISSS '12. New York, NY, USA: ACM, 2012, pp. 473–482. [Online]. Available: <http://doi.acm.org/10.1145/2380445.2380518>
- [44] D. Tămaş-Selicean and P. Pop, "Optimization of TTEthernet networks to support best-effort traffic," in *Proceedings of the 2014 IEEE Emerging Technology and Factory Automation (ETFA)*, Sept 2014, pp. 1–4.
- [45] G. Carvajal, C. W. Wu, and S. Fischmeister, "Evaluation of communication architectures for switched real-time ethernet," *IEEE Transactions on Computers*, vol. 63, no. 1, pp. 218–229, Jan 2014.